

states of EDA complexes^{17,19,20} provide evidence that an initially formed contact ion pair would rapidly relax to a solvent separated ion pair ($k_1 \approx 10^9 \text{ s}^{-1}$), which, in turn, would rapidly dissociate to free ions ($k_2 \approx 10^9 \text{ s}^{-1}$) in acetonitrile. Thus, within 2 ns most of the contact ion pairs in the present case might reasonably be expected to be converted to either solvent-separated ion pairs or to free ions. The conclusion that unencumbered radical anion or solvent-separated radical anion/cation are product-determining intermediates for the fragmentation processes observed is reinforced by our results in CTAB/ Et_3N where the radical anion is created as an unencumbered radical anion. The nearly exclusive formation of a single dehalogenated product in the reactions of LiDBB with penta-chlorobenzene and 1,2,3,5-tetrachlorobenzene at low temperatures is noteworthy. The fact that the expected major regioisomer can be predicted with precision allows for possible useful exploitation of this reaction.

Experimental Section

General Procedures. Reagent-grade acetonitrile (Baker Chemical Co.) was freshly distilled from phosphorus pentoxide, and its purity was greater than 99% by GLC analysis. The tetrahydrofuran used was freshly distilled from sodium benzophenone anion before each use. The lithium ribbon (Foote Mineral Co.) used for the radical anion reactions was >99%. Deionized, double-distilled water (potassium permanganate) was used in the micellar reactions.

General Procedure for Photolysis. All the samples for irradiation were prepared and irradiated as described earlier.²³ Micellar solutions were prepared by dissolving appropriate amounts of 1 in 0.2 M solution CTAB under vigorous stirring.

General Procedure for Radical Anion Reactions. The radical anions of naphthalene and *p,p'*-di-*tert*-butylbiphenyl

(DTBB) were prepared in THF according to the procedure described earlier.¹⁰ Typically, 20 mL of 0.05 M solution of DTBB (0.001 mol) in THF at the appropriate temperature was treated with 0.001 mol of lithium metal. After the mixture was stirred for 4 h, a solution containing 0.2 equiv of the halide in 1–2 mL of THF was syringed into the green radical anion solution of DTBB and purged with water after 10 min. In the case of pentafluorobenzene (15), 0.2 equiv of the radical anion solution, with respect to 6×10^{-4} mol of 15, was transferred under argon into a solution of 15 cooled to the appropriate temperature in order to minimize the formation of isomers other than 16–18.

Product Analysis. The photolysis mixtures were analyzed by GLC on a Varian 3300 capillary gas chromatograph equipped with an FID, a 30 m \times 0.25 mm DB-WAX capillary column (J & W Scientific Inc.) and a Varian 4290 integrator. The column was held at 60 °C for 5 min and raised to 180 °C at a rate of 5 °C/min with an injection port temperature of 200 °C and a detector temperature of 250 °C. Helium was used as carrier gas at 30 mL/min.

The reaction mixtures from micellar irradiations were extracted with pentane after dilution of the soapy solution. The recovery efficiency was typically ~90%. The product ratios were analyzed as in the previous text. Dodecane and hexadecane were used as internal standards.

The products from the radical anion reductions were analyzed after extracting the products from the THF–water mixture with pentane (recovery efficiency 85–90%) under the GLC conditions described previously. The pentane and residual THF were removed in a rotary evaporator before analysis. However, 15 and the products thereof were analyzed under different conditions. The extreme volatility of these aromatic fluorides necessitated the removal of pentane in a spinning band column. The removal of the residual THF, however, was not possible under these circumstances. The capillary column used to analyze the ratio of products was a combination of a DB-5 and DB-WAX (both 30 m \times 0.25 mm). The GLC column conditions for this analysis employed the following column temperature program: 30 °C for 35 min and raised to 180 °C at a rate of 20 °C/min with injection and detector temperatures as in the previous text.

Acknowledgment. Support of this research by the National Institute of Environmental Health Sciences (Grant ES00040) is gratefully acknowledged.

(17) Mataga, N.; Okada, T.; Kanda, Y.; Shioyama, H. *Tetrahedron* 1986, 42, 6143.

(18) Weller, A. Z. *Phys. Chem. Neue Folge* 1982, 130, 129.

(19) Gould, I. R.; Moody, R.; Farid, S. J. *Am. Chem. Soc.* 1988, 110, 7242.

(20) Goodman, J. L.; Peters, K. S. *J. Phys. Chem.* 1986, 90, 5506.

MM2 Model for the Intramolecular Additions of Acyl-Substituted Radicals to Alkenes

Jeffrey L. Broecker and K. N. Houk*

Department of Chemistry and Biochemistry, University of California, Los Angeles, Los Angeles, California 90024

Received August 10, 1990

The modified MM2 force field devised earlier to calculate transition states for intramolecular radical additions (Spellmeyer, D. C.; Houk, K. N. *J. Org. Chem.* 1987, 52, 959) has been extended to include acyl-substituted radicals. Calculations of the regioselectivities and stereoselectivities of the radical cyclizations are in good agreement with experimental results. The calculations show that the C(acyl)–C(rad)–C(alkene) attack angle and the geometric preference for planarity of the C(O)CH₂• radical, which is maintained in the transition structures for additions, cause the regioselectivities of acyl-substituted radical cyclizations to differ from those of alkyl radical cyclizations.

Introduction

Intramolecular additions of radicals to carbon–carbon double bonds to form five- and six-membered rings is a topic of intense current interest in synthetic organic chemistry.^{1–5} Such cyclizations are usually kinetically

controlled.¹ The 5-hexenyl radical cyclizes with high regioselectivity⁴ to give the five-membered ring (5-*exo* clo-

(3) (a) Beckwith, A. L. J.; Ingold, K. V. In *Rearrangement in Ground State and Excited States*; de Mayo, P., Ed.; Academic: New York, 1980; pp 162–283. (b) Beckwith, A. L. J. *Tetrahedron* 1981, 37, 3973. (c) Surzur, J. M. In *Reactive Intermediates*; Abramovitch, R. A., Ed.; Plenum: New York, 1981; Vol. 2, Chapter 3. (d) Griller, D.; Ingold, K. V. *Acc. Chem. Res.* 1980, 13, 317.

(4) Beckwith, A. L. J.; Easton, C. J.; Serelis, A. K. *J. Chem. Soc., Chem. Commun.* 1980, 482.

(1) Curran, D. P.; Chang, C.-T. *J. Org. Chem.* 1989, 54, 3140.
(2) Curran, D. P. *Synthesis* 1988, 417. Curran, D. P. *Synthesis*, 1988, 489.

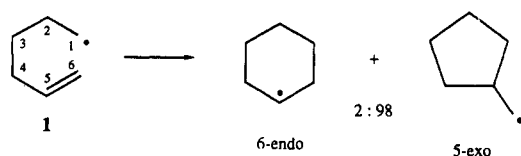


Figure 1. Regioselectivity of the cyclization of the 5-hexenyl radical.

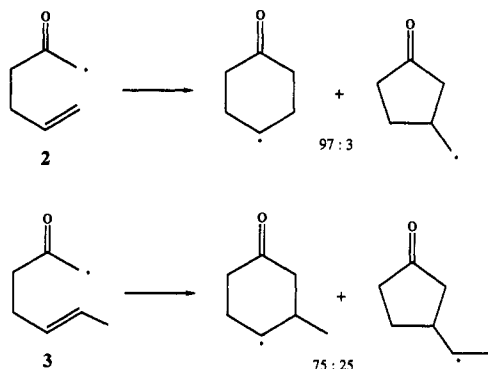


Figure 2. Regioselectivities of the cyclizations of 2-oxo-5-hexenyl and 2-oxo-5-heptenyl radicals.

sure) rather than the six-membered ring (6-*endo* closure) as is shown in Figure 1. Substituted 5-hexenyl radicals will normally cyclize to give 5-*exo* closure rather than 6-*endo* closure except when substituents at C-5 sterically retard 5-*exo* closure.²

The regiochemical control for this reaction has been attributed to electronic and steric effects.^{3a,3b,6,7} An MM2 force field was developed⁶ that models the transition states of this cyclization and correctly predicts the regiochemistries and stereochemistries of reaction products.

In striking contrast, intramolecular cyclizations of acyl-substituted radicals with the carbonyl part of the forming ring tend to close predominantly by the 6-*endo* pathway.^{1,8,9} As shown in Figure 2, the 2-oxo-5-hexenyl radical (2) cyclizes to give a 6-*endo*/5-*exo* ratio of 97/3; the 2-oxo-5-heptenyl radical (3) closes with an 6-*endo*/5-*exo* ratio of 75/25. Thus, 6-*endo* cyclization predominates even when there is steric hindrance to attack at C-6.

Curran,¹ Clive,⁸ and Porter⁹ have suggested that this reversal of regiochemistry arises from the resonance stabilization of the acyl-substituted radical; this alters the geometry of the radical and consequently the transition state as well. In order to investigate this regiochemical control, the alkyl radical addition MM2 force field⁶ has been extended to include acyl-substituted radicals. This paper presents the development and application of the force field model to acyl-substituted radical cyclizations. The force field permits prediction of regioselectivity and stereoselectivity of such reactions and facilitates understanding of the factors that contribute to regiochemical control in these systems.

Results and Discussion

Development of the Force Field. This force field has been developed to permit the calculation of the relative

energies of different conformations of transition states for additions of acyl-substituted radicals to alkenes. Since direct spectroscopic and theoretical data are not available for the transition states of these reactions, parameters for this force field were developed by modeling the experimental 6-*endo*/5-*exo* product ratios for the cyclizations of 2-16. These *endo*-*exo* ratios are indeed an indirect measurement of the energetics of the transition states since the reactions have been shown to be kinetically controlled.¹ This force field is a completely "flexible model" in which all atoms are free to move and are optimized in the calculation. Standard MM2 parameters¹⁰ are used for atoms not involved in the bond-formation or bond-breaking process. Atoms involved in this process are given new atom types 30 and 28, shown in the following structure, so that new parameters must be developed for bond lengths, bond angles, and torsional angles involving these atoms. Many



of the transition state parameters, listed in Appendix I, were taken directly from the alkyl radical addition parameter set.⁶ These parameters were developed from geometries and energies obtained by *ab initio* calculations on the transition states for additions of alkyl radicals to alkenes.^{6,11} For example, a forming bond length of 2.27 Å has been found for the transition state of the addition of methyl radical to ethylene.¹¹ Thus, the equilibrium bond length parameter for the force field is assigned a value of 2.27 Å. Parameters not included in the Spellmeyer-Houk parameter set, but newly developed for this force field, are discussed in the following text.

The equilibrium bond lengths for the 3-7 and 30-3 bonds were assigned values of 1.27 and 1.40 Å, respectively, on the basis of an experimental geometry of the formylmethyl radical ($\bullet\text{CH}_2\text{C}(=\text{O})\text{H}$).^{12,13} The experimental barrier for rotation about the bc bond of $\text{CH}_3\text{C}(\text{O})\text{CH}_2\bullet$, shown in the following structure, has been determined to be 9.4 kcal/mol.¹⁴ For substituted acetyl derivatives and ester-substituted ethyl radicals, the experimental barriers range from 8 to 15 kcal/mol.¹⁵ The MM2 torsional parameters assigned for rotation about this type of bond give an MM2 rotational barrier of 15.6 kcal/mol for rotation about the bc bond of $\text{CH}_2\text{C}(\text{O})\text{CH}_2\bullet$. The 15.6 kcal/mol parameters result in an overestimation of the difference in energy between the $\phi_r = 0$ and $\phi_r = 90$ conformers, but these parameters reproduce relative energies of the $\phi_r = 0$ and $\phi_r = 40$ conformations, which is the range for this torsional angle in the transition states of 2-16. In any case, the 15.6 kcal/mol parameters give a better fit to the experimental data for the regiochemistry of radical closure for 2-16 than do parameters that would give a

(5) Julia, M. *Acc. Chem. Res.* 1971, 4, 386. Julia, M. *Pure Appl. Chem.* 1974, 40, 553.

(6) Spellmeyer, D. C.; Houk, K. N. *J. Org. Chem.* 1987, 52, 959.

(7) Giese, B. *Angew. Chem., Int. Ed. Engl.* 1983, 22, 753. Giese, B. *Angew. Chem., Int. Ed. Engl.* 1985, 24, 553. Delbecq, F.; Ilavsky, D.; Anh, N. T.; Lefour, J. M. *J. Am. Chem. Soc.* 1985, 107, 1623. Poblet, J. M.; Candell, E. *Can. J. Chem.* 1983, 61, 2068.

(8) Clive, D. L. J.; Cheshire, D. R. *J. Chem. Soc., Chem. Commun.* 1987, 1520.

(9) Porter, N. A.; Cheng, V. H.-T.; Magnin, D. R.; Wright, B. T. *J. Am. Chem. Soc.* 1988, 110, 3554.

(10) MM2 Quantum Chemistry Program Exchange, 1980, 395. Allinger, N. L. *J. Am. Chem. Soc.* 1977, 99, 8127. Allinger, N. L. *Adv. Phys. Org. Chem.* 1976, 13, 1.

(11) Houk, K. N.; Paddon-Row, M. N.; Spellmeyer, D. C.; Rondan, N. G.; Nagase, S. *J. Org. Chem.* 1986, 51, 2874.

(12) Dimauro, L. F.; Heaven, M.; Miller, T. A. *J. Chem. Phys.* 1984, 81, 2339.

(13) Dupuis, M.; Wendoloski, J. J.; Lester, W. A., Jr. *J. Chem. Phys.* 1982, 76, 488.

(14) Kochi, J. K. In *Adv. Free-Radical Chem.*; Vol 5, Williams, G. H., Ed.; Academic Press: New York, 1975; Vol. 5, p 255. Golde, G.; Mobius, K.; Kaminski, W. *Z. Naturforsch.* A 1969, 24, 1214.

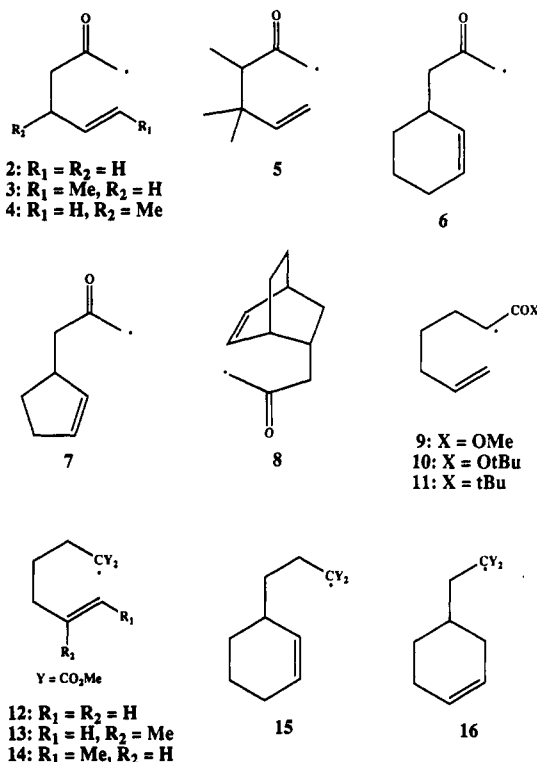
(15) Struh, W.; Roduner, E.; Fischer, H. *J. Phys. Chem.* 1987, 91, 4379. Lung-min, W.; Fischer, H. *Helv. Chim. Acta* 1983, 66, 138.

Table I. Regiochemical Ratios for Intramolecular Radical Cyclizations

radical	<i>endo/exo</i>	
	calculated (ΔE)	experimental ($\Delta\Delta G$) ^a
2	95:5 (2.0)	97:3 (2.3) ^a
3	68:32 (0.5)	75:25 (0.7) ^a
4	97:3 (2.4)	only <i>endo</i> (>2.5) ^b
5	99:1 (3.0)	91:9 (1.6) ^a
6	0:100 (-4.2)	only <i>exo</i> (<-2.5) ^a
7	1:99 (-3.1)	only <i>exo</i> (<-2.5) ^b
8	0:100 (-3.6)	only <i>exo</i> (<-2.5) ^b
9	12:88 (-1.4)	7:90 (-1.7) ^a
10	9:91 (-1.6)	6:94 (-1.9) ^a
11	15:85 (-1.2)	25:75 (-0.8) ^a
12	8:92 (-1.6)	10:90 (-1.5) ^a
13	92:8 (1.7)	only <i>endo</i> (>2.5) ^a
14	0:100 (-5.2)	only <i>exo</i> (<-2.5) ^a
15	0:100 (-6.5)	only <i>exo</i> (<-2.5) ^a
16	3:97 (-2.3)	only <i>exo</i> (<-2.5) ^a

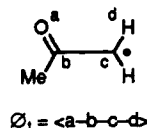
^aReference 1, 70 °C. ^bReference 8, 80 °C.

lower barrier to rotation about this bc bond.¹⁶ For example, parameters ($V_1 = 0$, $V_2 = 1.70$, $V_3 = 0$; for X-30-3-Y type atoms) that result in a 4.5 kcal/mol barrier for rotation about the bc bond in $\text{CH}_3\text{C}(\text{O})\text{CH}_2\cdot$ show an 0.8 kcal/mol preference for *exo* cyclization for compound 2 and a 2.3 kcal/mol preference for *exo* cyclization for 3. Calculations with parameters ($V_1 = 0$, $V_2 = 3.6$, $V_3 = 0$; for X-30-3-Y type atoms) that result in a 9.4 kcal/mol rotational barrier for $\text{CH}_3\text{C}(\text{O})\text{CH}_2\cdot$ favor *endo* closure by 1.0 kcal/mol for 2 and favor *exo* closure by 0.6 kcal/mol for 3. As shown in Table I, the parameters used in this



paper ($V_1 = 0$, $V_2 = 6.25$, $V_3 = 0$; for X-30-3-Y atom types) favor *endo* cyclization for 2 by 2.0 kcal/mol and *endo* closure for 3 by 0.5 kcal/mol. Thus, the MM2-calculated ratio for *endo/exo* cyclization is very sensitive

to the magnitude of the rotational barrier about the 30-3 bond, such that an increase in this barrier of 4-5 kcal/mol favors *endo* closure over *exo* closure by 1-2 kcal/mol.



The 3-30-28-1 torsional parameters were assigned values of $V_1 = 0.0$, $V_2 = 0.0$, and $V_3 = 1.139$. These parameters lead to slightly higher rotational barriers among the 60 and 180° conformers of the transition state than the analogous Spellmeyer-Houk parameters for the 1-30-28-1 torsional angle ($V_1 = 1.364$; $V_2 = -1.103$; $V_3 = 0.339$). This increased barrier for 3-30-28-1 favors 1-6 closure over 1-5 for radicals 9-16 by 0.5-1.0 kcal/mol because the torsional angles about the 30-28 bond for 1-6 closure for these radicals are only ~3-5° away from a staggered configuration, while the torsional angles about this bond for 1-5 closure are 30-50° away from staggered. As an example, calculations on compounds 9 and 10 using the values of $V_1 = 0.0$, $V_2 = 0.0$, and $V_3 = 1.139$ for the 3-30-28-1 parameter favor 6-*endo* closure by 1.0 kcal/mol more than calculations using the Houk-Spellmeyer values of $V_1 = 1.364$, $V_2 = -1.103$, and $V_3 = 0.339$ for this 3-30-28-1 parameter. Radicals 1-8 are relatively unaffected by this increased barrier, as the 30-28 torsional angles are within 10° of a staggered conformation for both 1-5 and 1-6 closure.

Locations of the Transition States. The transition states for 5-*exo* or 6-*endo* closure of radicals 1-16 were located by minimizing the energy with respect to all the parameters involved in bond formation and bond breaking. The unusually long bonds in the bond-forming and bond-breaking process of the transition states have been defined as minima in our force field by choosing unusually long equilibrium bond distance parameters (e.g., 30-28 = 2.27 Å). Thus, the transition states were located in the same manner as ground states are found in normal MM2 calculations. Care should be taken using this force field to avoid modeling transition states in which the bond-breaking and bond-forming process deviate significantly from that of the transition states of the basis set of compounds (2-16) used to develop this force field. The number of possible conformations of the forming ring is small; consequently, the searches for all possible conformations of the transition states were done manually by beginning with all reasonable conformers. Several transition states were usually found for each 5-*exo* or 6-*endo* ring closure for radicals 1-16. In these cases, the energy difference between 5-*exo* and 6-*endo* ring closure was determined from a Boltzmann distribution over all transition states that have energies within 2 kcal/mol of the transition state of lowest energy.

Regiochemical Control. The calculated and experimental 6-*endo*/5-*exo* ratios for radicals 1-16 are listed in Table I. The MM2 results and the experimental results are in good agreement. The results show that radicals 2-5 all favor 6-*endo* cyclization. This reversal of regiochemical control in the acyl-substituted radical cyclizations compared to the alkyl radical cyclizations can be understood by a close examination of the MM2 transition states for the cyclizations of the 2-oxo-5-hexenyl radical. Two transition states of equal energy were found for 5-*exo* closure, a chairlike transition state (Figure 3) and the boatlike transition state (Figure 4). Similar transition states were found earlier for the 5-*exo* cyclizations of the 5-hexenyl radical.⁶ However, in that case the boat tran-

(16) Ab initio UHF/6-31G* calculations also overestimate the magnitude of this rotational barrier as calculations on the planar and twisted conformations of $\cdot\text{CH}_2\text{C}(\text{O})\text{H}$ showed a 13.8 kcal/mol barrier for rotation about this $\cdot\text{CH}_2\text{C}(\text{O})$ bond. Results are detailed in the supplementary material.

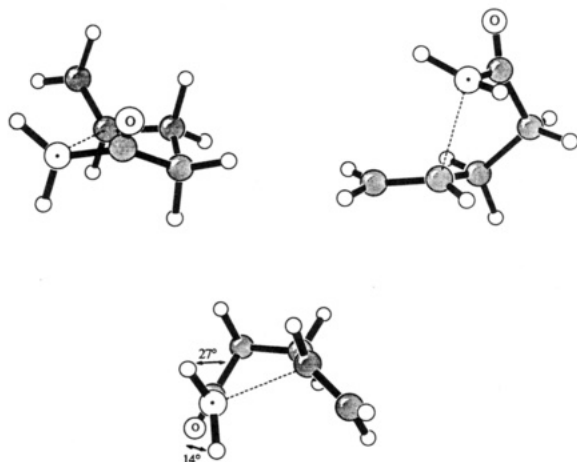


Figure 3. Three views of the chair transition structure for the 5-*exo* cyclization of **2**.

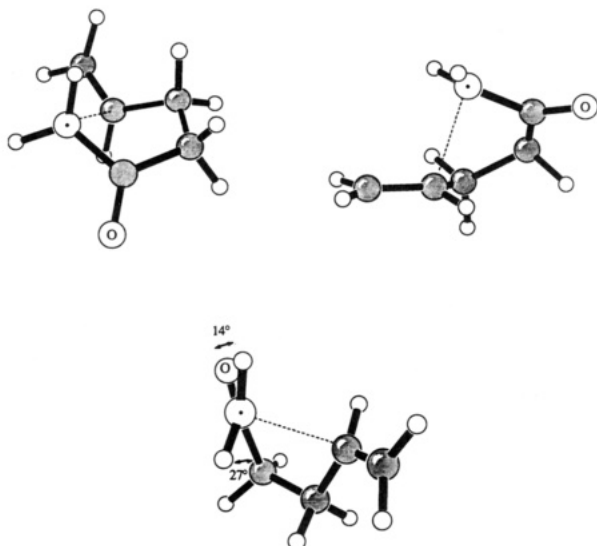


Figure 4. Three views of the boat transition state structure for the 5-*exo* cyclization of **2**.

sition state is 0.5 kcal/mol higher in energy than the chair. The boat and chair transition states of **2** are closer in energy because of the steric interaction between the alkene double bond and the forming ring in the chair transition state, as shown in Figure 3. In the chair conformation, the alkene type 2 carbon atom is an average of 0.4 Å closer to the carbonyl carbon and the alkyl carbons of the forming ring than it is to these atoms in the boat conformation. This results in approximately a 0.5 kcal/mol destabilization of the chair conformer relative to the boat. A chair transition state (Figure 5) was found for 6-*endo* closure. This is 2.5 kcal/mol lower in energy than the 5-*exo* transition states. A 6-*endo* boat transition state was also found, but it was 5 kcal/mol higher in energy than the endo chair. The most important factor that destabilizes *exo* closure versus *endo* closure is the torsional strain about the C-(acyl)-C(rad) bond, along with the C(acyl)-C(rad)-C(alkene) attack angle strain in the 5-*exo* transition state. The third view in Figures 3–5 shows the C(acyl)-C(rad) torsional angles. The H-C(rad) hydrogen atoms are twisted off planarity in the *exo* transition states by averages of 14 and 27°, which is significantly more than the *endo* transition state, where these values are 5 and 22°. This increased twisting destabilizes the *exo* transition states by 1.7 kcal/mol. The C(acyl)-C(rad)-C(alkene) angle also favors 6-*endo* closure. Ab initio calculations indicate that this angle is 100° in the transition states of the alkyl radical

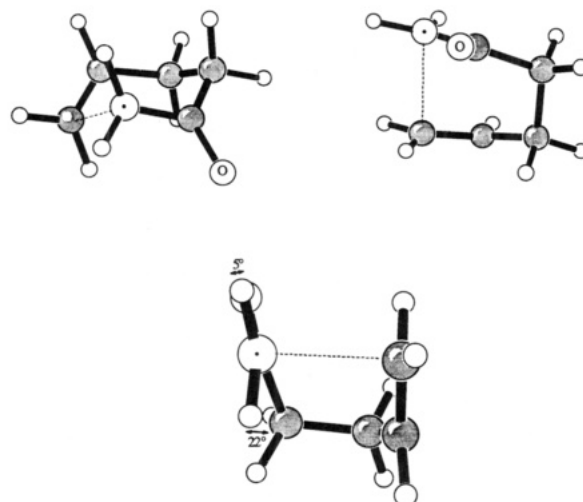


Figure 5. Three views of the chair transition state structure for the 6-*endo* cyclization of **2**.

attack on alkenes in the absence of ring strain.¹¹ The MM2 calculations for radical **2** show that 6-*endo* closure forces this angle to close to 89° in the transition state. The 5-*exo* closure forces the angle to be 83°, which amounts to a 1.6 kcal/mol destabilization of 5-*exo* closure versus 6-*endo* closure.

Beckwith proposed that the preference for 5-*exo* closure for alkyl radical attack on alkenes is related to C(rad)-C(alkene)-C(alkene) bond angle distortion in the 6-*endo* transition state.^{3a,b} This has been reproduced by force field calculations.⁶ Ab initio calculations show that this angle is 107° when unstrained.¹¹ While this angle is readily achieved for the 5-*exo* transition state for radical **1**, this angle can be achieved only with considerable strain in the transition state for 6-*endo* cyclization. In the 6-*endo* transition state this angle is 96°, which accounts for 1.9 kcal/mol additional strain in the endo transition state. This type of angle strain is also present in the cyclization of the 2-oxo-5-hexenyl radical. The C(rad)-C(alkene)-C(alkene) bond angle for 5-*exo* closure is 108°, while this bond angle for 6-*endo* closure is 97°. This difference in angle strain favors the 5-*exo* closure by 1.4 kcal/mol. In the case of the cyclization of 2-oxo-5-hexenyl radical, this 1.4 kcal/mol is overwhelmed by the C(acyl)-C(rad) torsional effect (1.7 kcal/mol) and the C(acyl)-C(rad)-C(alkene) angle effect (1.6 kcal/mol), both of which favor *endo* closure. These three factors (1.7 + 1.6 - 1.4 = 1.9) account for most of the 2.4 kcal/mol destabilization of the 5-*exo* transition states versus the 6-*endo* transition state for radical **2**.

Cyclizations of radicals **4** and **5** give similar 6-*endo*/5-*exo* ratios as **2**, since all three radicals have basically the same steric effects for 5-*exo* closure and 6-*endo* closure. Cyclization of radical **3**, however, results in relatively more 5-*exo* product than **2**, **4**, or **5** because the methyl group at C-6 sterically inhibits 6-*endo* closure. The calculations also show that the additions of radicals to cyclic alkenes (radicals **6**–**8**) overwhelmingly favor 5-*exo* cyclization in agreement with the experimental results. This is due to bending strain and 1,4 van der Waals interactions; both strongly disfavor *endo* cyclizations of these radicals. Finally, the cyclizations of radicals **9**–**16** follow the pattern of alkyl radical cyclizations: 5-*exo* closure is generally favored over 6-*endo* closure, again in good agreement with experimental results. In these radicals, the acyl group is now external to the forming five- or six-membered rings. This allows the C(acyl)-C(rad) torsional angle and the C(acyl)-C(rad)-C(alkene) angle to achieve their optimal

Table II. Stereochemical Ratios for Intramolecular Radical Cyclizations by 5-*exo* Closure

radical	<i>cis/trans</i>	
	calculated (ΔE)	experimental ^a ($\Delta\Delta G$)
9	46:54 (-0.11)	50:40 (0.15)
10	48:52 (-0.05)	44:49 (-0.07)
11	46:54 (-0.11)	27:73 (-0.68)

^a Reference 1, 70 °C.

values without strain in either the *endo* or *exo* closure. Thus, radicals 9–16 generally give *exo* closure except when C-5 is sterically hindered.

As was mentioned earlier, the C(acyl)–C(rad)–C(alkene)–C(alkene) torsional parameter was crucial in fitting the calculated *exo/endo* ratios to the experimental data for radicals 9–16. This torsional parameter was hardened (larger energy barrier to rotation from 60–180 °C) compared to the analogous Spellmeyer–Houk parameter. This will not change the results of any calculations for alkyl radical cyclizations using the Spellmeyer–Houk parameter set, since only the 3–30–28–1 parameter was changed. This alteration may be necessary due to the increased steric bulk about the attacking radical in compounds 9–16. Alternatively, in the cases of 12–16 the transition state may be later because of the increased electrophilic nature of the radical as has been suggested by Curran.¹ The increase in rotational barrier for this torsional parameter may be necessary to properly account for this later transition state.

Stereochemical Control. Table II lists the three radicals (9–11) for which experimental stereochemical data is available. The calculations predicted that 5-*exo* closure should give roughly equal mixtures of *cis* and *trans* products, in agreement with experimental data. Radical 11 shows the worst deviation with a 0.7 kcal/mol preference for the *trans* isomer found experimentally but only a 0.1 kcal/mol preference for the *trans* isomer calculated. The formation of *cis* product has also been found to compete with *trans* product in alkyl radical cyclizations.⁶

Computational Methods

Molecular mechanics calculations were performed with Allinger's MM2(82) program¹⁰ modified to include equivalence of certain atom types.⁶ The standard MM2(82) parameters used in this work are unchanged in the MM2(85) force field. The new parameters developed in this work are given in the Appendix.

Conclusions

The MM2 force field developed for acyl-substituted radical cyclizations gives results that are in good agreement with experimental data. The calculations showed that 6-*exo* cyclization is favored over 5-*exo* cyclization when the acyl group is part of the forming ring. The losses of resonance of the acyl radical and increased angle strain in the forming ring disfavor 5-*exo* closure.

Acknowledgment. We acknowledge helpful discussions with Professors Dennis Curran and Derrick Clive. We are grateful to the National Institutes of Health for financial support of this research.

Appendix

The radical center in the transition state is defined as atom type 30, while the alkene carbon atom undergoing attack is defined as atom type 28. The remaining carbon of the double bond stays as atom type 2. Atom types 30 and 28 were set equivalent to atom type 1; that is, all parameters for atom types 30 and 28 not defined are assigned values equal to the analogous parameters for atom

type 1. For example, bond length parameters for bond type 30–1 are set equal to bond length parameters for bond type 1–1.

Torsional parameters:

atom type				V ₁	V ₂	V ₃
30	28	2	1	0.00	–25.00	0.00
30	28	2	5	0.00	–25.00	0.00
5	2	28	5	0.00	0.00	0.25
5	2	28	1	0.00	0.20	0.20
1	2	28	5	0.00	0.00	0.34
1	2	28	1	0.40	0.03	0.50
3	30	28	1	0.00	0.00	1.139
3	30	28	5	0.00	–0.003	0.0273
5	30	28	5	0.00	0.00	0.0267
1	30	28	5	0.00	0.00	0.0273
5	30	28	2	0.00	0.00	0.0405
5	30	28	1	0.00	0.00	0.0646
1	30	28	2	–0.241	0.241	0.399
1	30	28	1	1.364	–1.103	0.339
5	1	2	28	0.00	0.00	–0.24
1	1	2	28	–0.44	0.24	0.06
28	30	3	7	0.00	0.00	0.00
28	30	3	1	0.00	0.00	0.00
28	30	3	5	0.00	0.00	0.00
5	30	3	5	0.00	6.25	0.00
5	30	3	7	0.00	6.25	0.00
5	30	3	1	0.00	6.25	0.00
1	30	3	1	0.00	6.25	0.00
1	30	3	5	0.00	6.25	0.00
1	30	3	7	0.00	6.25	0.00
1	30	3	6	0.00	6.25	0.00
5	30	3	6	0.00	6.25	0.00
3	30	3	6	0.00	6.25	0.00
3	30	3	1	0.00	6.25	0.00
3	30	3	5	0.00	6.25	0.00
3	30	3	7	0.00	6.25	0.00
3	6	1	2	–2.03	1.21	–0.67

Stretching parameters:

bond type	K(S)	L(O)
30–28	4.00	2.27
28–2	4.40	1.38
30–7	4.40	1.40
3–7	10.3	1.27

Bending parameters:

atom types			K(B)	$\theta(O)$
5	30	5	0.32	116.60
5	30	28	0.36	100.50
30	28	5	0.36	90.30
30	28	2	0.60	107.00
5	28	2	0.36	120.3
5	28	5	0.32	115.8
28	2	5	0.36	121.40
5	2	5	0.32	117.0
1	30	5	0.36	116.6
1	30	1	0.45	116.6
1	30	28	0.45	100.5
30	28	1	0.45	90.3
1	28	2	0.45	120.3
1	28	5	0.36	115.8
1	28	1	0.45	115.8
28	2	1	0.45	121.4
5	2	1	0.36	117.0
3	30	5	0.32	116.6
30	3	7	0.40	121.9
30	3	1	0.40	119.40
30	3	5	0.39	117.8
30	3	6	0.65	111.35
3	30	3	0.45	116.6
3	30	28	0.45	100.5
3	30	1	0.45	116.6

Supplementary Material Available: Ab initio calculations on HC(O)–CH₂ (3 pages). Ordering information is given on any current masthead page.